



## **Trade Studies on best source and best fusion method for global DTED2 over the CEOS-WGCV-TMSG test sites**

Jan-Peter Muller  
Point of Contact **GEO Task DA-07-01**  
Chair, CEOS-WGCV Terrain mapping Sub-Group  
Mullard Space Science Laboratory  
University College London  
Holmbury St. Mary  
Dorking  
Surrey  
RH5 6NT, UK

Draft v1 (31 March 2008)

### **Abstract**

ASTER 30m DEMs were provided by NASA over 4 CEOS-WGCV-TMSG test sites: Aix-en-Provence, Barcelona, Three Gorges and Puget Sound. We report here on experiments to assess the best method to (a) merge the most cloud-free single 30m ASTER DEMs with 90m SRTM to create a 30m DEM over the Three Gorges; (b) merge a stack of ASTER DEMs by cloud clearing using a fixed threshold over Aix-en-Provence; (c) merge a stack of ASTER DEMs by pre-screening for water and cloud features using an existing DEM over Barcelona. In each case, independent “ground truth” DEMs were employed to assess the quality of the input ASTER DEMs and their fused derivative products. It should be noted that for one of the test areas, Aix-en-Provence, unknown datum effects meant that there was a spatially variant shift between the “ground truth” and the spaceborne DEMs whatever their source. Overall, ASTER DEMs only just meet the DTED-2® accuracy requirements, The compliance depends critically on how effective the compositing method is with regards to the complete removal of cloud contamination. An algorithm is outlined which could be employed to identify *ab initio* obscuring features such as clouds. However, water features will still need to be identified as the heights of these features can vary from one ASTER-DEM to another.

### **Context**

The creation of a global 30m DEM is one of the stated goals of the GEO task (DA-07-01)<sup>1</sup>. Ideally, this 30m DEM would be created using the format specification of the US DoD/NGA called DTED® level 2 (1 arc-second grid-spacing, 16m 90% LE= 12m Zrms). In 2000, SRTM acquired such a dataset for some 80% of the Earth’s land-mass. A variety of analyses (e.g. Weydahl, D. J., Sagstuen, J., Dick, O. B., and Ronning, H., 2007) show that the SRTM DEM in many areas meet or exceed the SRTM-2® specification. However, aside from the conterminous US (lower 48 states) where such DEM data is available, the SRTM DTED-2® has not been released due to constraints caused by the

---

<sup>1</sup> Muller, J-P. (2008) GEOSS Interoperability Guidance on DEM data. Version 1, 21 March 2008, 27pp

data policies of US allies (NGA, private communications, 2005-7). Also, some authors (Guth, P. L., 2006; Kelindorfer, J., 2007) have questioned whether these datasets are truly 1 arc-second when several studies have indicated that as a result of SAR speckle filtering, the resolution is more likely to be around 2 arc-seconds. However, even if SRTM-DTED-2® were publicly available, there would still be around 2-3% gaps within the region from 60°N to 56°S. These gaps or voids result from radar topographic shadows, layover or due to penetration in dry desert sands. They can be brute-force filled using existing DEM data sources and increasingly sophisticated feathering/merging techniques or 3<sup>rd</sup> party DEM sources can be employed to fill the gaps (Grohman, G., Kroenung, G., and Strebeck, J., 2006; Reuter, H. I., Nelson, A., and Jarvis, A., 2007). An alternative source, which up until recently was difficult to access due to the very high cost that the sensor owners have placed on the derived products are DEMs derived from ASTER. The SilCAST software (Fujisada, H., Bailey, G. B., Kelly, G. G., Hara, S., and Abrams, M. J., 2005) allows DEMs to be routinely and rapidly produced from input ASTER along-track stereo-pairs. This software has been installed at the US Geological Survey's EROS Data Center (EDC) since June 2006. Through an online ordering system, it is possible to acquire tens of ASTER DEMs with only a few hours turnaround time period. One of the reasons why this is possible is that the DEM extraction process is fully automated and one of the reasons why this is the case is that the accuracy of the exterior and interior orientation is sufficiently high that "dead reckoning" can be employed to transform the stereo-matched disparities into 3D positions on the surface of the Earth.

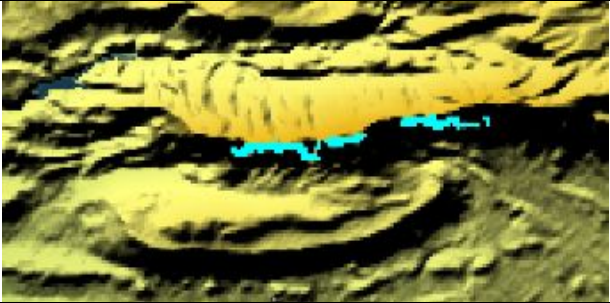



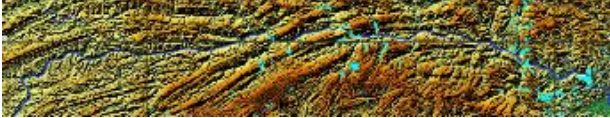
### **Aims and Objectives**

To best assess what data sources will meet the requirements to provide global and consistent DTED2® (30m) data, a small number of trade studies were performed consisting of:

1. Assessing the error characteristics of each spaceborne DEM dataset which is available for a given area using the "ground truth" DEMs available
2. Assessing the practicality of using multiple coverages to beat down cloudy data and/or phase unwrapping errors to improve accuracy through multiple dataset averaging
3. Assessing the best method of data fusion for one or more datasets to eliminate clouds (stereo-optical) and data gaps caused by radar shadows or occlusions or very dry soil moisture conditions

### **CEOS-WGCV-TMSG Test sites**

The Committee on Earth Observing Satellites (CEOS) was set up in 1987 as a result a G7 summit in Paris. CEOS has 3 Working Groups of which the WGCV (Working Group on Cal/Val) is the most long established. As well as national space agency representations, there are 6 Sub-groups of which the "Terrain Mapping from satellites SG" (TMSG) is one of the most active. The author has chaired the TMSG since 2001 and prior to this he was an active member since 1996. In addition to the development of a manual of best practise and keeping abreast of current developments in the creation and validation of spaceborne DEMs, TMSG maintains an active list of cal/val sites. Table 1 lists the current TMSG sites which have been established over the last 12 years. They also show what the DEM looks like and briefly summarise what ancillary datasets are available for validation and what issues there are for each site.

Short-name	Extent (lon)	Extent (lat)	Validation datasets	ICEDS WMS image
Aix-en-Provence  Europe (F)	5.528-5.685°E	43.502-43.560°N	Aerial top-of-canopy Pitkin DEM (UCL), DTM (IGN)	
Barcelona  Europe (ES)	1.5-2.75°E	41.25-41.82°N	Aerial top-of-canopy DEM (ICC)	
North Wales  Europe (UK)	-3 to -5°W	52-53.5°N	OS® 50m DTM kGPS	
Puget Sound  WA (USA)	-121.397 to -123.897°W	46.364-48.864°N	NED 30m DTM Lidar 2m top and bottom of canopy DEM	
Three Gorges Asia (China)	108.252-111.302°E	30.638-31.229°N	CASM 50m DTM, kGPS	

**Table 1. Current portfolio of CEOS-WGCV TSMG test-sites including coloured hill-shaded DEMs derived from the SRTM (V2, edited) layer of ICEDS (<http://iceds.ge.ucl.ac.uk>)**

### Merging ASTER and RTM DEMs to try to create a DTED-2® like product

As part of a larger study conducted under the aegis of the ESA-NRSCC DRAGON programme, Nick Austin (the 2006 ESA DRAGON prizewinner) looked at a range of different methods with the author of fusing 90m SRTM-DTED-1® DEM with ASTER 30m DEM data.

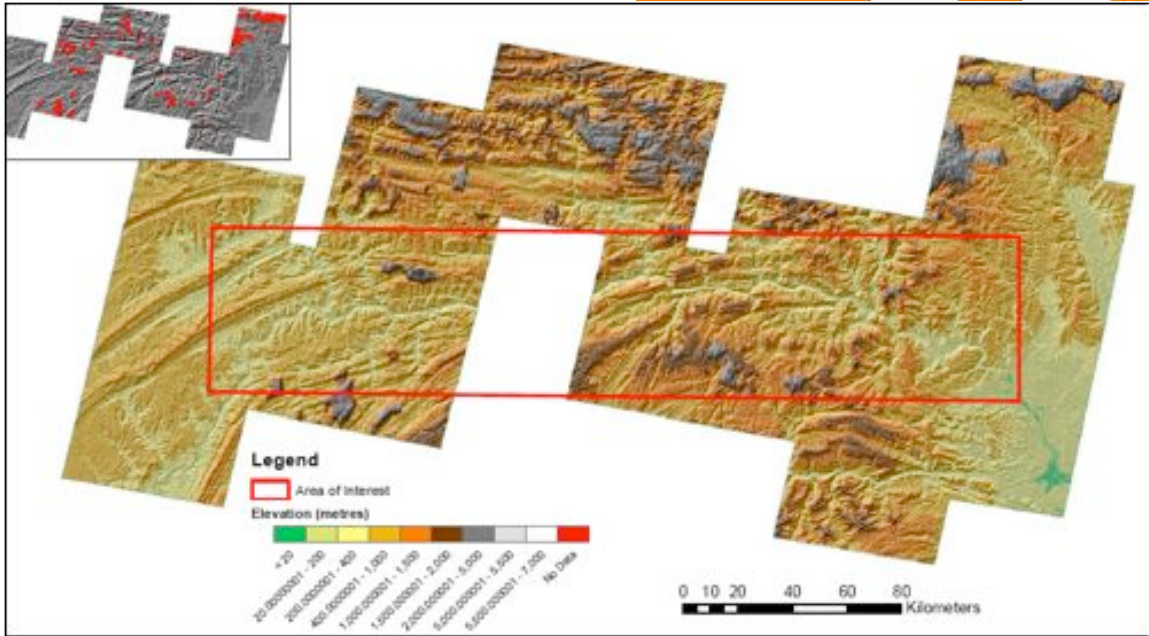
Thirteen ASTER DEMs were obtained from near cloud-free images. Their basic details are contained in Table 2.

Data Granule	Date Acquired	Geographic Centre
SC:AST_L1A.003:2009403469	05/05/2000	30.88° Lat, 109.99° Lon
SC:AST_L1A.003:2006428272	12/05/2000	31.35° Lat, 109.05° Lon
SC:AST_L1A.003:2006428292	12/05/2000	30.81° Lat, 108.90° Lon
SC:AST_L1A.003:2006563192	21/05/2000	30.81° Lat, 110.50° Lon
SC:AST_L1A.003:2010420979	12/09/2000	30.84° Lat, 108.73° Lon
SC:AST_L1A.003:2006288948	08/03/2002	30.60° Lat, 108.11° Lon
SC:AST_L1A.003:2006288946	08/03/2002	31.13° Lat, 108.25° Lon
SC:AST_L1A.003:2008534198	25/09/2002	31.04° Lat, 110.49° Lon
SC:AST_L1A.003:2023324413	09/05/2004	30.45° Lat, 110.76° Lon
SC:AST_L1A.003:2023324413	09/05/2004	30.98° Lat, 110.90° Lon
SC:AST_L1A.003:2027019514	12/12/2004	30.60° Lat, 111.25° Lon
SC:AST_L1A.003:2027019515	12/12/2004	31.13° Lat, 111.38° Lon
SC:AST_L1A.003:2031440138	26/10/2005	31.46° Lat, 109.81° Lon

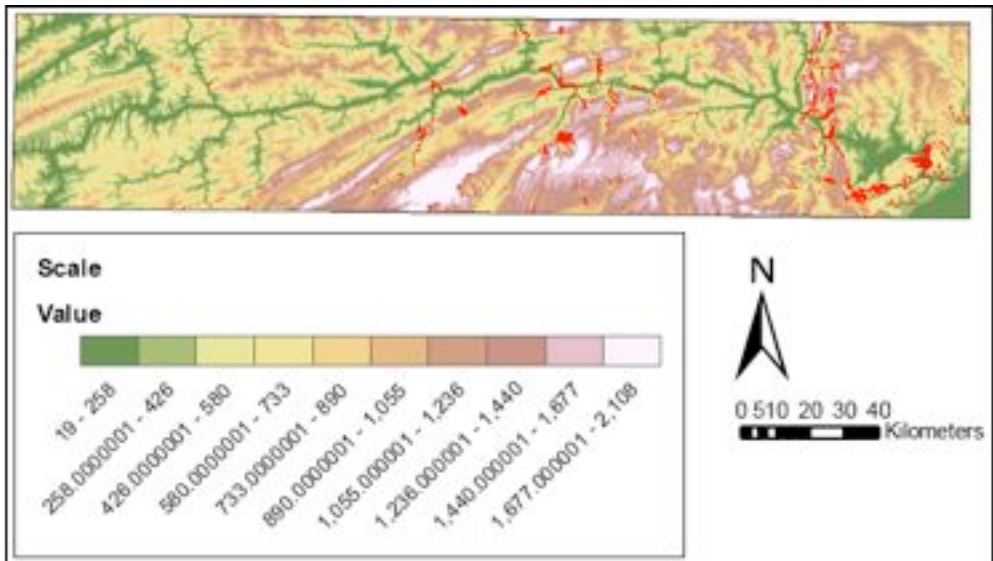
**Table 2. ASTER scenes employed in the ASTER-SRTM data fusion experiment.**

These ASTER DEMs were mosaiced together and are shown in Figure 1. This mosaic was then differenced from the corresponding SRTM DEM shown in Figure 2. The reader should note that there are areas in the ASTER DEM which are significantly higher than the corresponding SRTM DEM even given the factor of 3 difference in grid-spacing between ASTER and SRTM and that the ASTER DEM has missing areas where no cloud-free or near cloudfree ASTER DEM could be found and that the SRTM DEM contains significant gaps. This means that when fusing these 2 products we will land up with pixels which contain only ASTER DEM height, pixels with SRTM DEM heights and pixels which have had to be interpolated because neither ASTER or SRTM were available. Fortunately, the last of these 3 cases is hardly present within the scene.

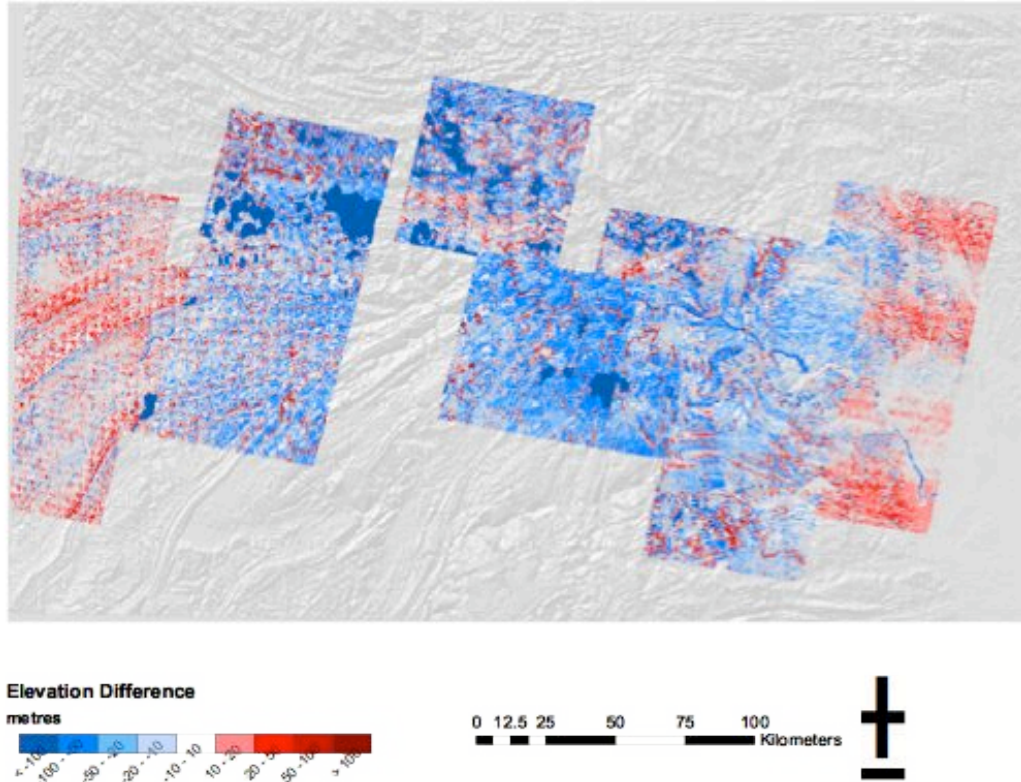
After checking that there was good planimetric co-registrtrion between the 2 DEMs, the SRTM was differenced from ASTER to yield the difference DEM shown in Figure 3. This shows that there is still a residual bias in each ASTER frame, probably due to orbital and/or pointing errors and in some areas of this DEM difference, there is a ripple effect indicating along-track attitudinal jitter which has been observed before in SPOT DEMs.



**Figure 1. ASTER DEM coloured by height and using a simple hill-shading model. Inset shows a greyscale version of the hill-shaded DEM with heights in red indicating heights which are above 100m threshold between ASTER and SRTM. After Austin, N. J., Muller, J.-P., Lixia, G., and Zhang, J (2008)**

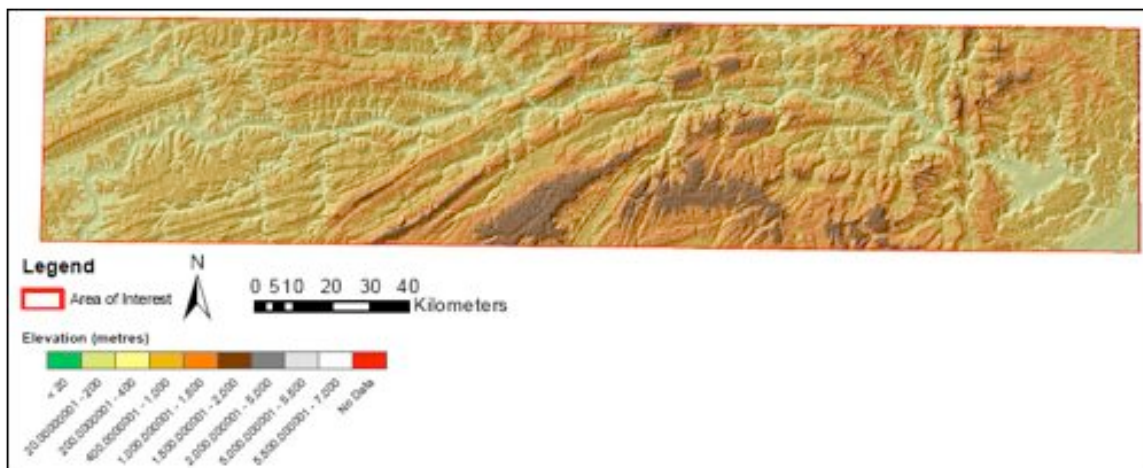


**Figure 2. SRTM DEM coloured by height over the area of interest. Approximately 2% of the area is missing (shown here in red).**

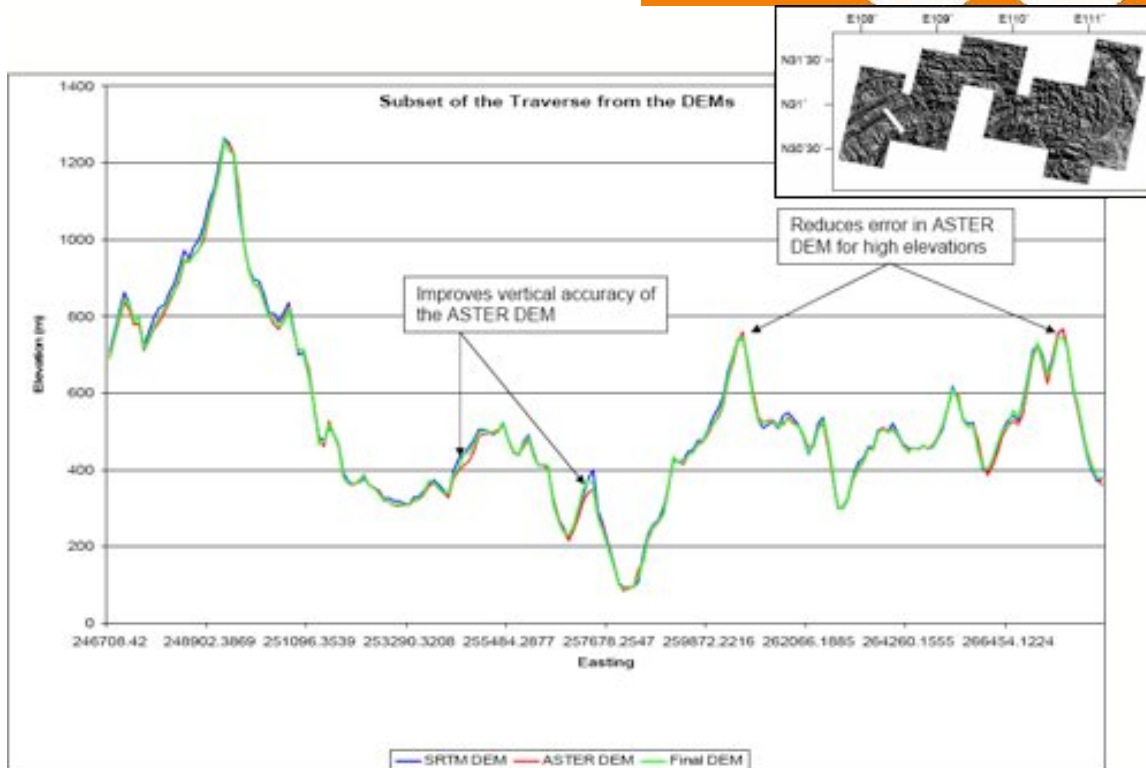


**Figure 3. SRTM minus ASTER DEM height differences. Note the differences in the overall bias of the DEMs (blue or red) and the significant banding shown.**

Several different methods were tested and the most successful used ER-mapper® algebraic functions to combine the DEMs. See Austin et al (2008) for details. Figure 4 shows the final DEM with all gaps filled whilst Figure 5 shows a comparison over a transect compared with 3<sup>rd</sup> party “ground truth”. This analysis concluded that the final bias was  $4.62 \pm 10.3\text{m}$  which is well within the DTED-2® specification.



**Figure 4. Final 30m fused ASTER-SRTM DEM.**

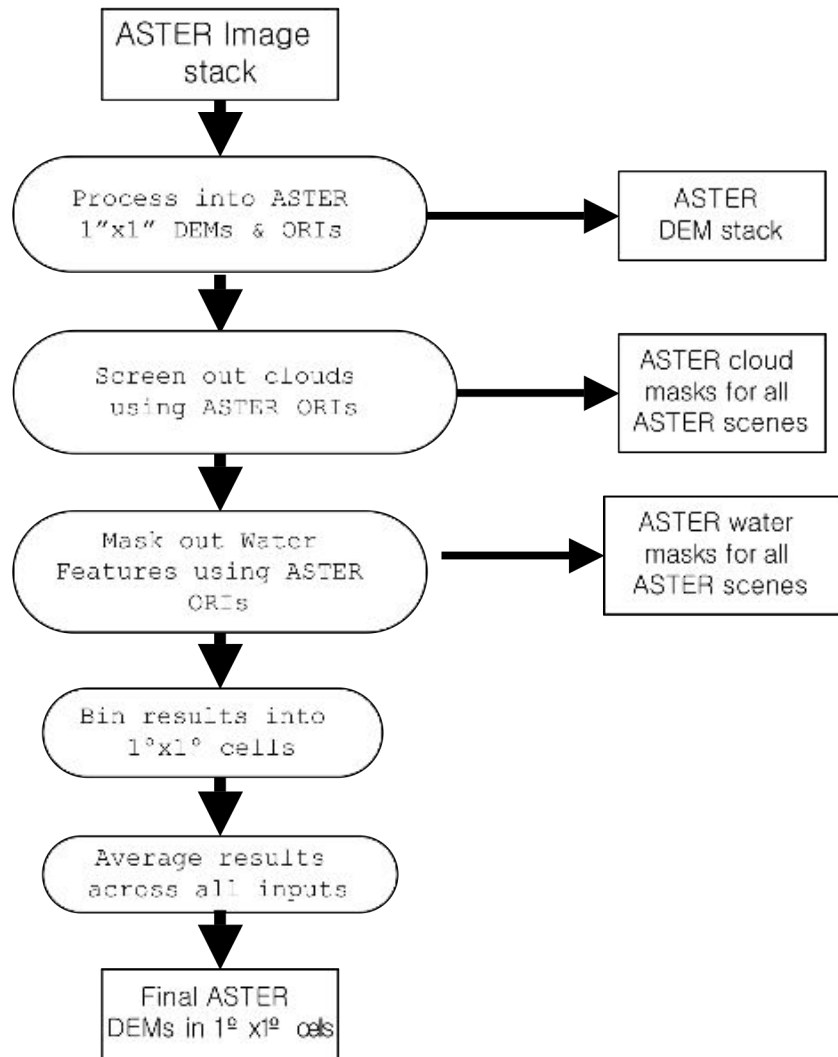


**Figure 5. SRTM, ASTER and fused DEM inter-comparison over the transect shown in the inset. ASTER tends to smooth out the hill-tops and SRTM suffers from slope-induced effects.**

Although this picture seems very encouraging, there are still issues which do not appear at the scale of the entire area. In particular, there are still residual clouds as sometimes their cloud-tops lie within the 100m threshold. It is therefore necessary to try to find a method of detecting these clouds.

### Data Processing Schematics for ASTER DEM stacking

In Muller (2008)<sup>2</sup>, the global 30m ASTER GDEM project is described. Although technical details of this project are not yet available, particularly concerning the exact methods employed, it is known that some 1.4 million ASTER scenes are being stereo matched and converted in DEMs using “dead reckoning”. Although an answer was not received from Dr Fujisada (who is in charge at SilCAST Corporation of the GDEM production), Dr Bryan Bailey (EDC) believes that there is a cloud screening process to remove cloud-top heights. I have shown what I believe may be the data processing schema in Figure 6 to create the 22,895 1° x 1° tiles of 1 arc-second ASTER-GDEMs.



**Figure 6. Schematic flowchart showing the ASTER GDEM production processing system as divined from discussions with Dr Brian Bailey (EDC)**

The quality of the final results will depend critically on (a) near perfect cloud-screening; (b) near perfect water body detection. Unfortunately, it is not feasible to repeat this

<sup>2</sup> Muller, J-P. (2008) GEOSS Interoperability Guidance on DEM data. Version 1, 21 March 2008, 27pp



process as both cloud detection and water body detection using ASTER ORIs are not sufficiently well developed at UCL to perform this routinely. In the last section of this report, a method is proposed for automatically compositing stacks of ASTER-DEMs without having to perform cloud detection. However, it was not possible to implement and test this to a sufficient degree prior to completion of this report.

Instead, a pragmatic set of methods have been employed consisting of 4 steps:

1. EITHER use a fixed height threshold for cloud-tops
2. OR difference the ASTER DEM heights from a 3<sup>rd</sup> party DEM and threshold the results to identify pixels which are likely to be non-ground
3. Set the thresholded “clouds” and “water body features” (e.g. from the ground truth DEM flags) to IEEE NaN (or set to MISSING DATA VALUE if geospatial processing system is available)
4. Perform statistics on this data stack to calculate mean, median, standard deviation, minimum and maximum heights

The overall process is shown schematically in Figure 7. The input ASTER uses a flag value of “-9999” to represent missing data whilst the ancillary DEM uses “0” and SRTM DEM uses “-32768”. All of these values had to be replaced by NaN after converting the original input integer DEMs (16-bit signed integers) to floating point.

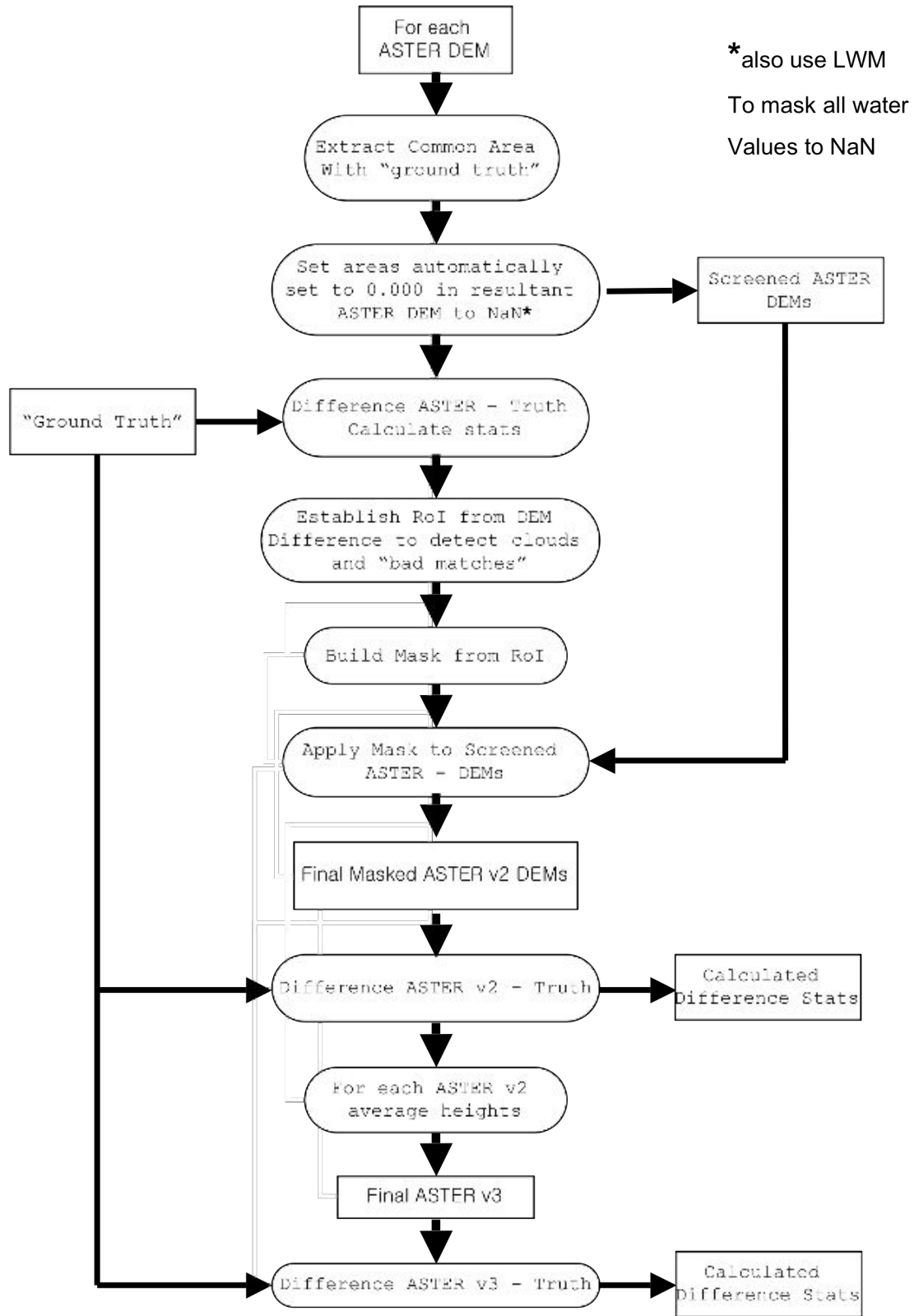
The key component for this process is the calculation of statistics of the data layer stack using either NaN or MISSING DATA VALUE(MDV) to ignore calculations if there is missing data. Unfortunately, neither ENVI/IDL nor ERDAS-IMAGINE are capable of dealing with MDV or handling NaN properly and so many days were wasted trying to work with this process. The same problems occurred on Mac, PC-Windows or PC-linux.

Unfortunately, these systems appear to work as if NaN is a mask so that if any of the input data stack has a NaN for a particular pixel in the stack, then the output of an averaging processing (i.e. sum all heights and divide by the number of layers in the stack) will be NaN instead of an average of the remaining frames by adjusting the number of input layers to divide the sum of all valid heights within the stack.

An IDL program was written which instead used the following logic:

- (a) for each pixel in the DEM stack
  - test if it is NaN
- (b) if NaN, skip that pixel
- (c) increment a counter of the number of pixels within the stack
- (d) move onto the next data layer and test if that pixel has a value of NaN
- (e) when the last data layer is reached, calculate the mean, median, minimum, maximum and standard deviation of the heights which have non-NaN values using the counter value and output the results

These results are shown later.



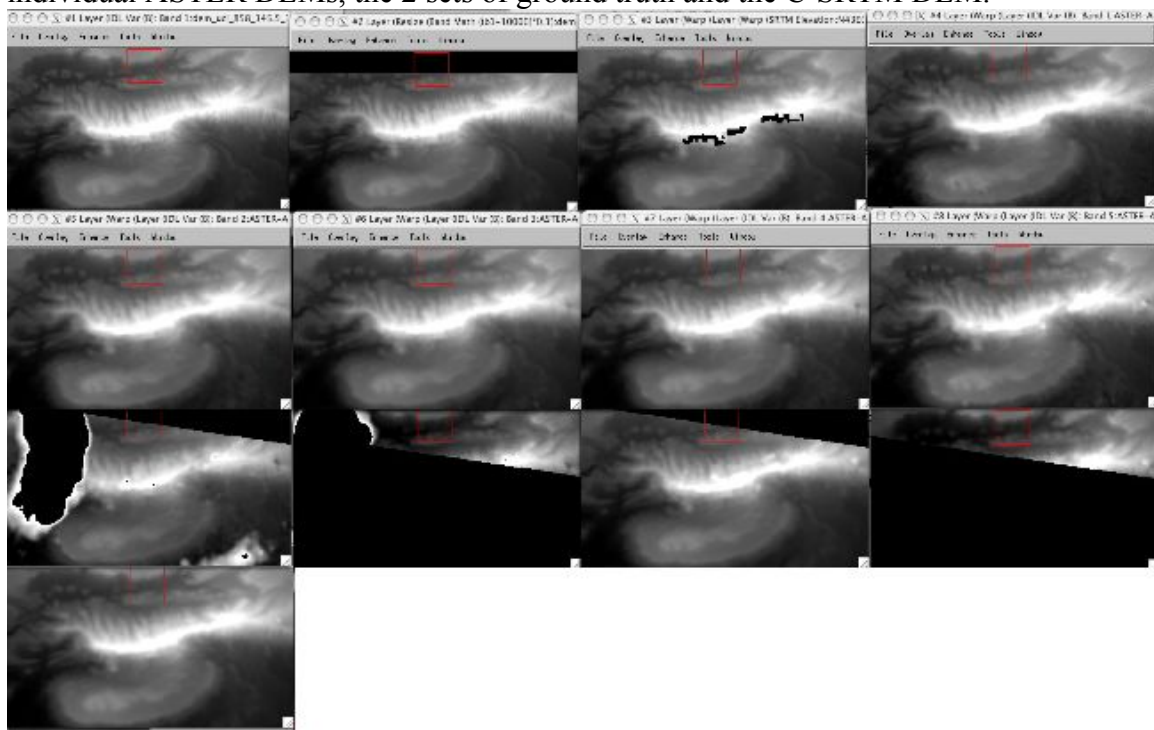
**Figure 7. Schematic diagram of pragmatic data processing scheme to reproduce some of the characteristics of the automated ASTER DEM production system.**

## Results

One of the most challenging aspects of this processing, which was not properly resolved, was the fact that the ASTER and SRTM DEMs were both georeferenced with respect to a gravity/water model called EGM96 whilst the horizontal co-ordinates were with respect to the WGS84 ellipsoid. Unfortunately, neither ENVI nor IMAGINE (the UK CHEST license for all HEIs for the ARCinfo® software expired during the completion of this work and has not yet been renewed due to ITAR issues) understand geoids and ellipsoids properly. For example, ENVI labels WGS84 a datum when this is an ellipsoid. This means that if the “ground truth” datasets are on a different datum from the spaceborne DEMs there will be spatially variant shifts which cannot be removed. In the case of the Aix-en-Provence DEMs, the datum is unknown. Therefore there was a spatially variable shift between the so-called Pitkin “ground truth” DEM which varied from ASTER scene to ASTER scene. One way of dealing with this is to use surface matching (Buckley, S. J. and Mitchell, H. L., 2004). However, a version of this software was not available. This means that the results for AeP should be viewed with scepticism.

### Aix-en-Provence : Fixed height threshold to remove clouds

In Appendix 1, individual scenes are displayed together with relevant information on their location and size. Although there were 14 ASTER DEMs, two were found to lie outside the area of interest, six had no missing data, two had substantial cloud contamination and four did not cover the entire area of interest. Figure 8 shows the individual ASTER DEMs, the 2 sets of ground truth and the C-SRTM DEM.



**Figure 8. Mosaic of 13 data layers within the DEM stack for the Aix-en-Provence test site. Upper-row: Pitkin-DEM, IGN-DEM, SRTM-DEM, 1<sup>st</sup> ASTER-DEM.**

Remaining rows ASTER-DEMs. For description see column labelled # for mapping in Appendix 1.

Note the missing data in the IGN, the voids on the ridge of the mountain in the SRTM and the imperfect removal of clouds using a threshold of 1060m just above the highest point within the mountain.

The 6 artefact-free ASTER DEMs were then averaged together (using ENVI) and the 12 ASTER DEMs which included 6 which contained NaN were processed using the algorithm described in the previous section. It should be noted that a shift can be observed (it is just around 1 pixel) using a false-colour composite of the Pitkin, IGN and SRTM (as R,G,B). These 3 have been added to the bottom of Figure 8 to create Figure 9 below.

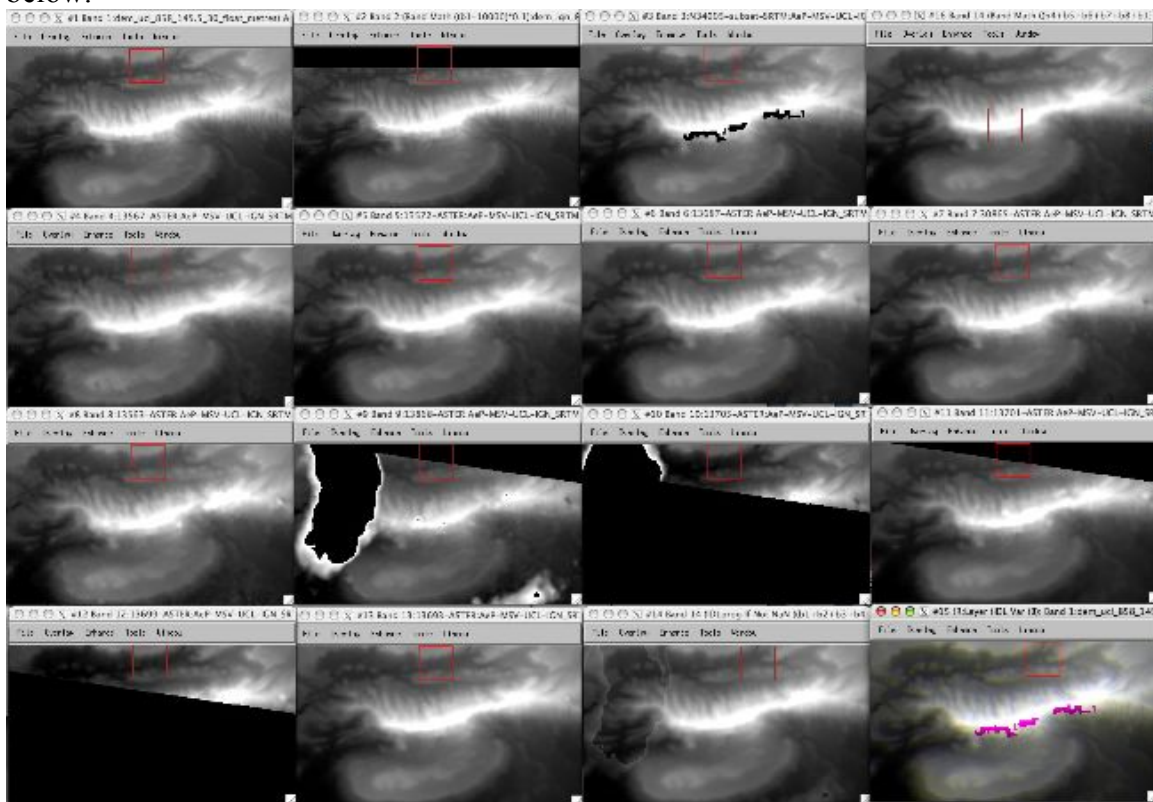
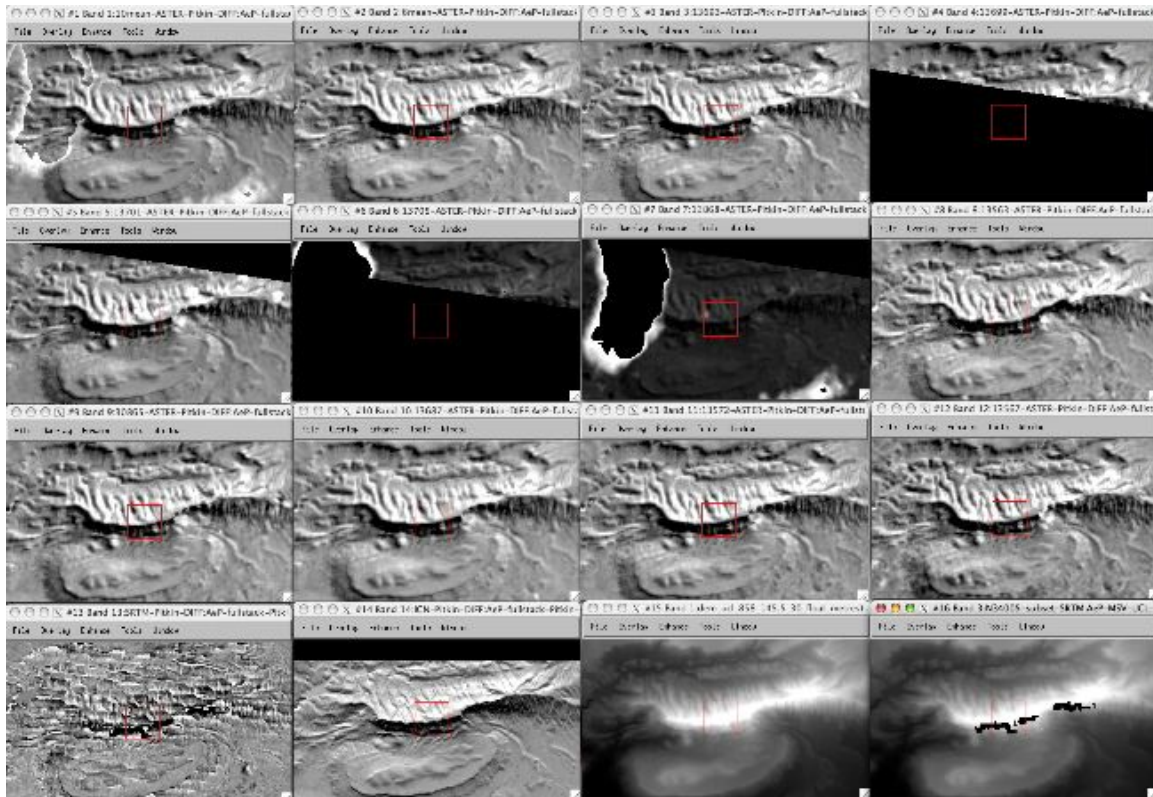


Figure 9. Same as Figure 3 with the addition of the 6-mean, 12-mean and FCC of the uppermost leftmost DEMs (Pitkin,IGN,SRTM=R,G,B).

Using the Pitkin DEM (as it was obtained at the canopy-top through manual photogrammetry) as the “truth”, difference DEMs (dDEMs) were processed for each of the 14 pairings. The statistics as well as the histograms are shown in Figure 10. The difference images mostly look like hill-shaded representations with the exception of the SRTM-Pitkin DEM difference. The reason for this is the small but significant planimetric shift between the different DEM pairings. Note the lack of such a shift for the SRTM which looks well co-registered with the Pitkin DEM. Although it is not visible here, by

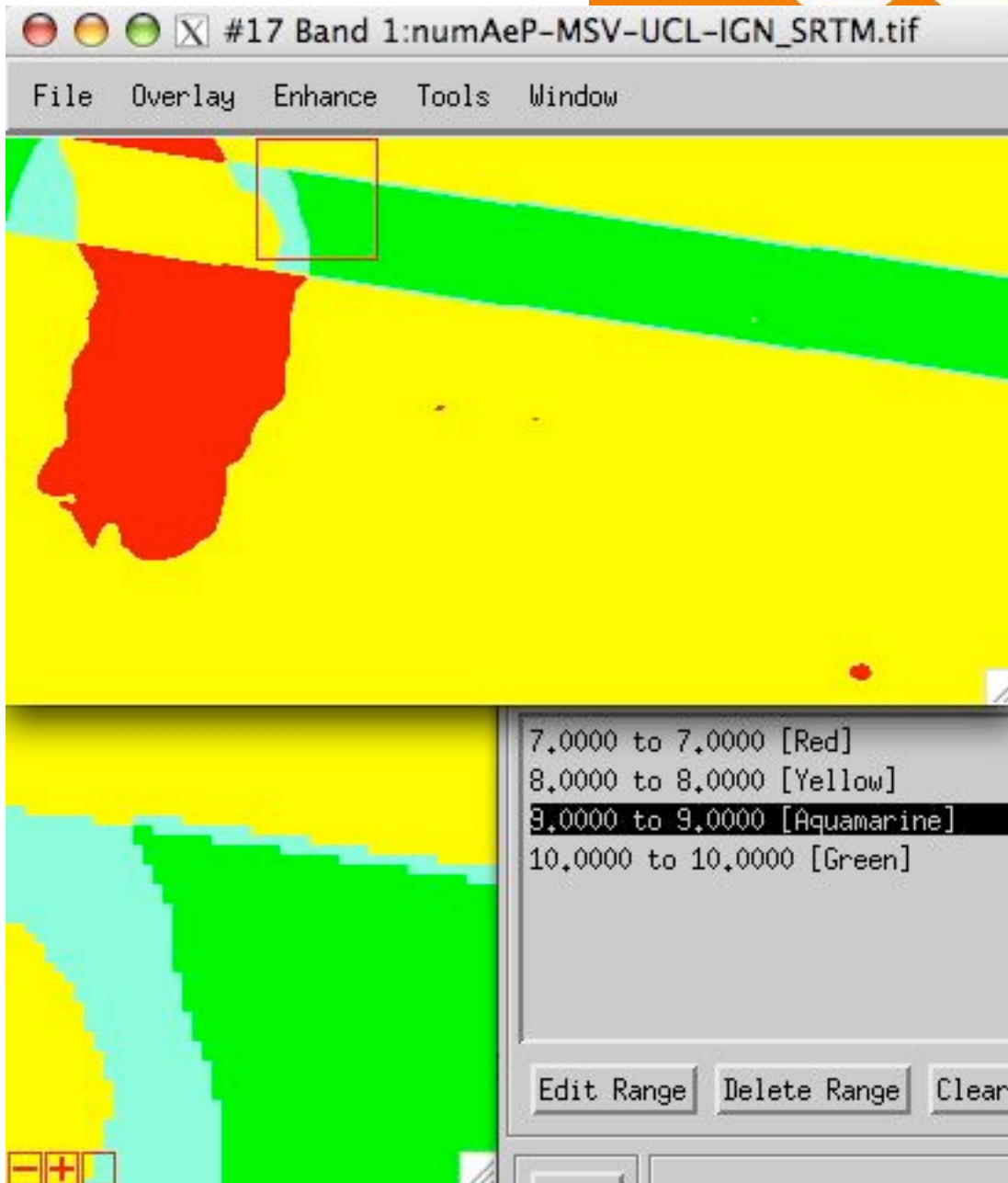
flickering between the different DEMs, it was noted that there was almost perfect co-registration ( $\leq 1$  pixel) between all the ASTER DEMs.



**Figure 10. DEM differences between 12mean, 6mean and all the individual ASTER DEMs, followed by the SRTM-UCL and the IGN-UCL DEM difference images. The original Pitkin DEM and SRTM DEM are shown in the last rightmost position.**

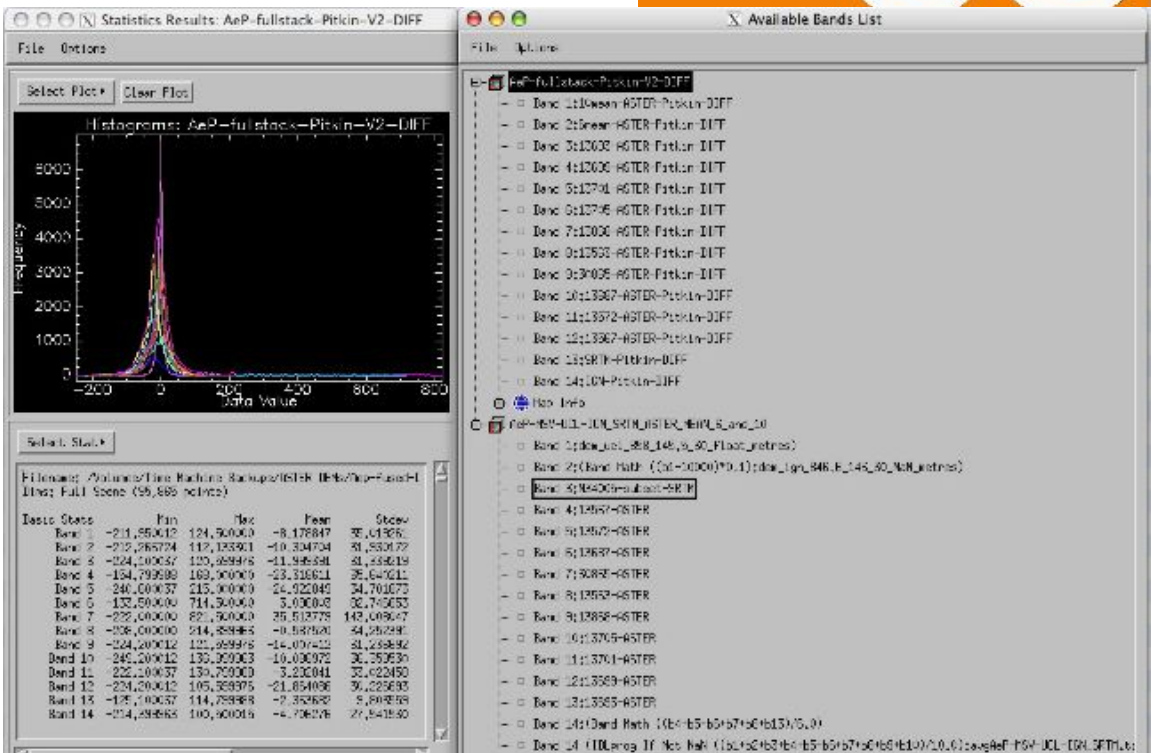
The best DEM is the 6mean of the cloud-free DEMs. The 12mean of all the DEMs shows the dramatic impact of the cloud-screened area in the 3<sup>rd</sup> from the left, 2<sup>nd</sup> from top DEM. Figure 11 shows the count for the individual DEM grid-points including the complex patterns around one of the cloud thresholded sections. You can observe that the reason for the apparent cloud threshold area appearing in the composite of the 12mean DEM is that there are 2 other missing sections in this area which conspire together to produce a poor average.

The ASTER DEMs were chosen from the set which had a cloud fraction  $< 5\%$ . Hence for this test site, there was only a maximum of 10 points per grid-points. Following discussions with Bryan Bailey (EDC), the ASTER-GDEM project envisage that if all ASTER DEMs are used which are not completely cloud-covered then there could be up to 50 points per DEM grid-point. However, this does rely on near-perfect cloud detection and removing all scenes which contain aerosol hazes. Only validation of the final DEM products will be able to tell if these have had any impact on the final DEM quality.



**Figure 11. Coverage map showing the number of pixels used to create the 12-mean DEM. Note the appearance of the masked-out cloud. See text for details.**

Histograms and the raw statistics for the DEM differences are shown in Figure 12 below. Note the poor standard deviation (mostly around 35m) and the very large range (up to  $\approx 800\text{m}$ ) due to imperfect removal of clouds. Only the SRTM DEM comes close to the DTED-2<sup>®</sup> specification ( $\leq 12\text{m}$  Zrms). However, as discussed above, this is most likely due to the poor co-registration of the ground truth Pitkin DEM with all the other DEMs due to the lack of knowledge of the datums.



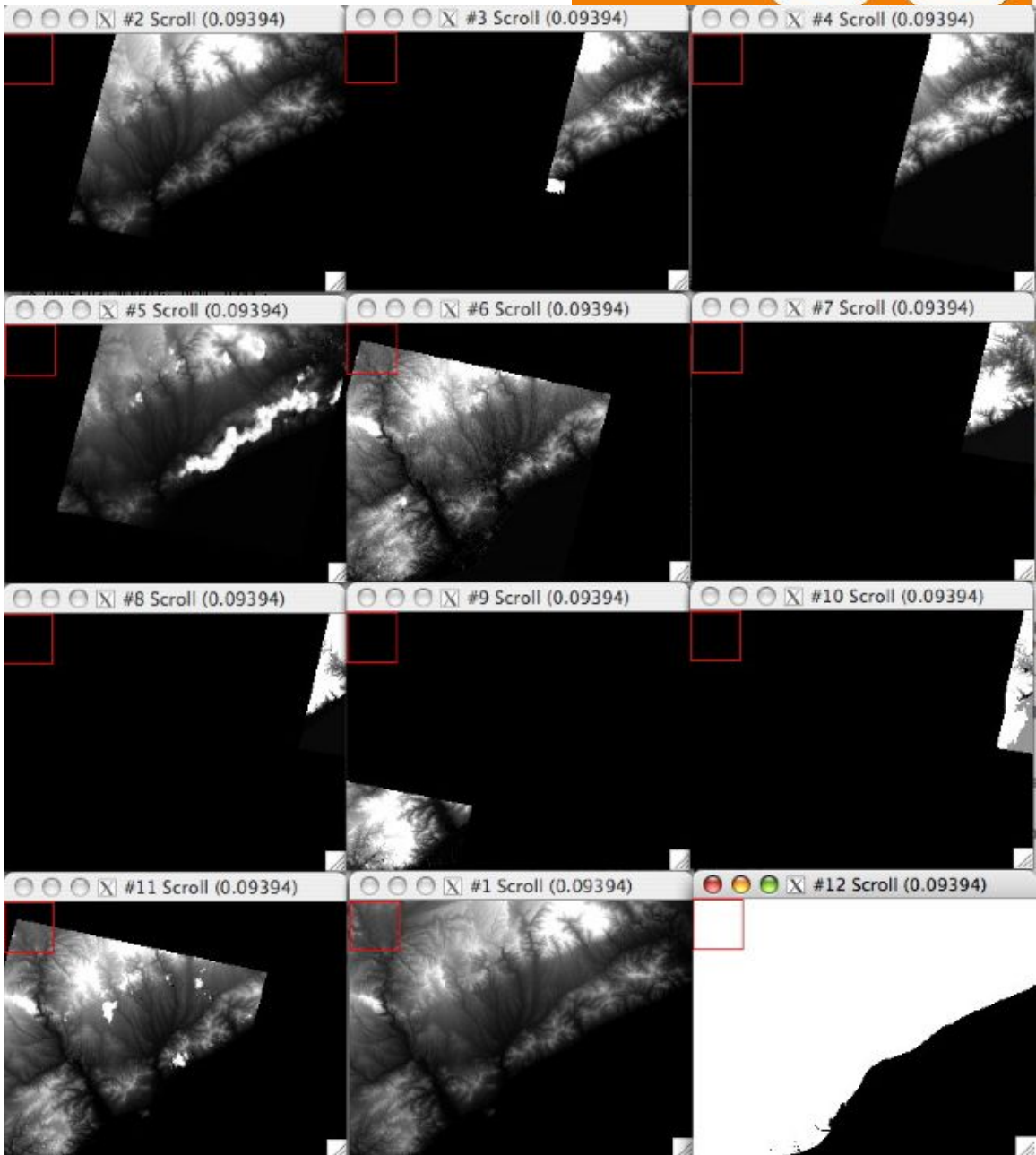
**Figure 12. DEM-Pitkin difference statistics including histograms, and overall statistics for each individual DEM. Note the large bias for most the DEM difference pairings due to the planimetric shift between the ASTER and “ground truth” DEMs.**

Barcelona: Use of 3<sup>rd</sup> party DEM to remove clouds, pits and water features

To try to understand better how sensitive the ASTER compositing process is to the near perfect correction for clouds and water features, a set of 10 ASTER DEMs were employed for a variety of tests.

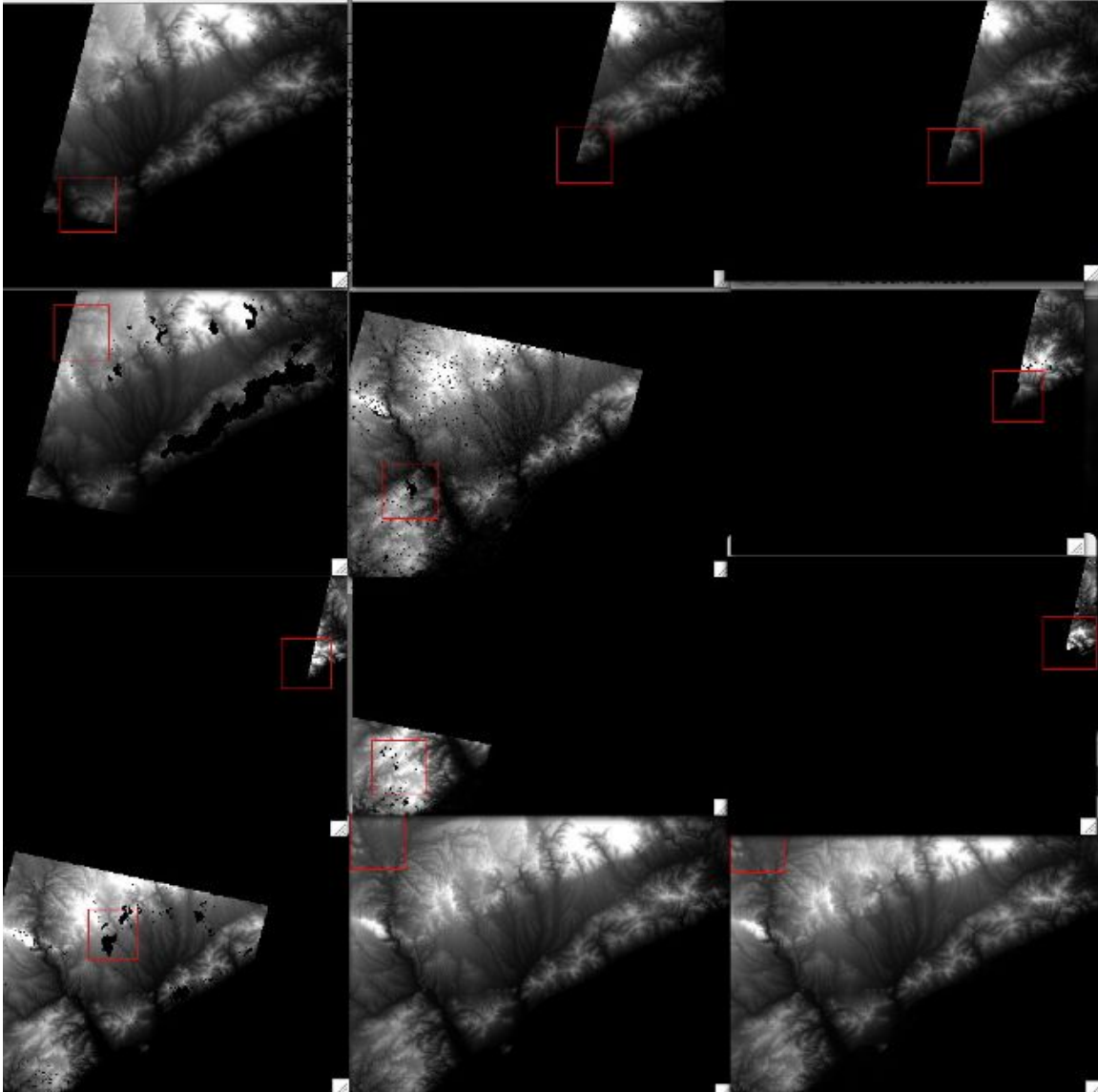
Firstly, the individual DEMs are shown in Appendix 2 together with relevant georeferencing information. Ten of the DEMs were selected as being within the test area. These DEMs together with the reference DEM from ICC and the derived land-water mask (LWM) are shown in Figure 13.

Applying the LWM mask and a variable threshold individually tuned by hand for the ASTER-Pitkin elevation difference to maximise the detection of clouds, pits due to cloud shadow or integer round-off error, the set of inputs for the average elevation is shown in Figure 14 together with the SRTM DEM for the whole area.



**Figure 13. Individual ASTER DEMs (See Appendix 2 for details), the “ground truth” photogrammetrically-derived DEM and the LWM derived therefrom.**





**Figure 14. Cloud-screened and stereo-matcher pit artefact screened DEMs which form the inputs to the averaging process. Reference DEM from ICC and SRTM (C-band) DEM in lower right corner.**

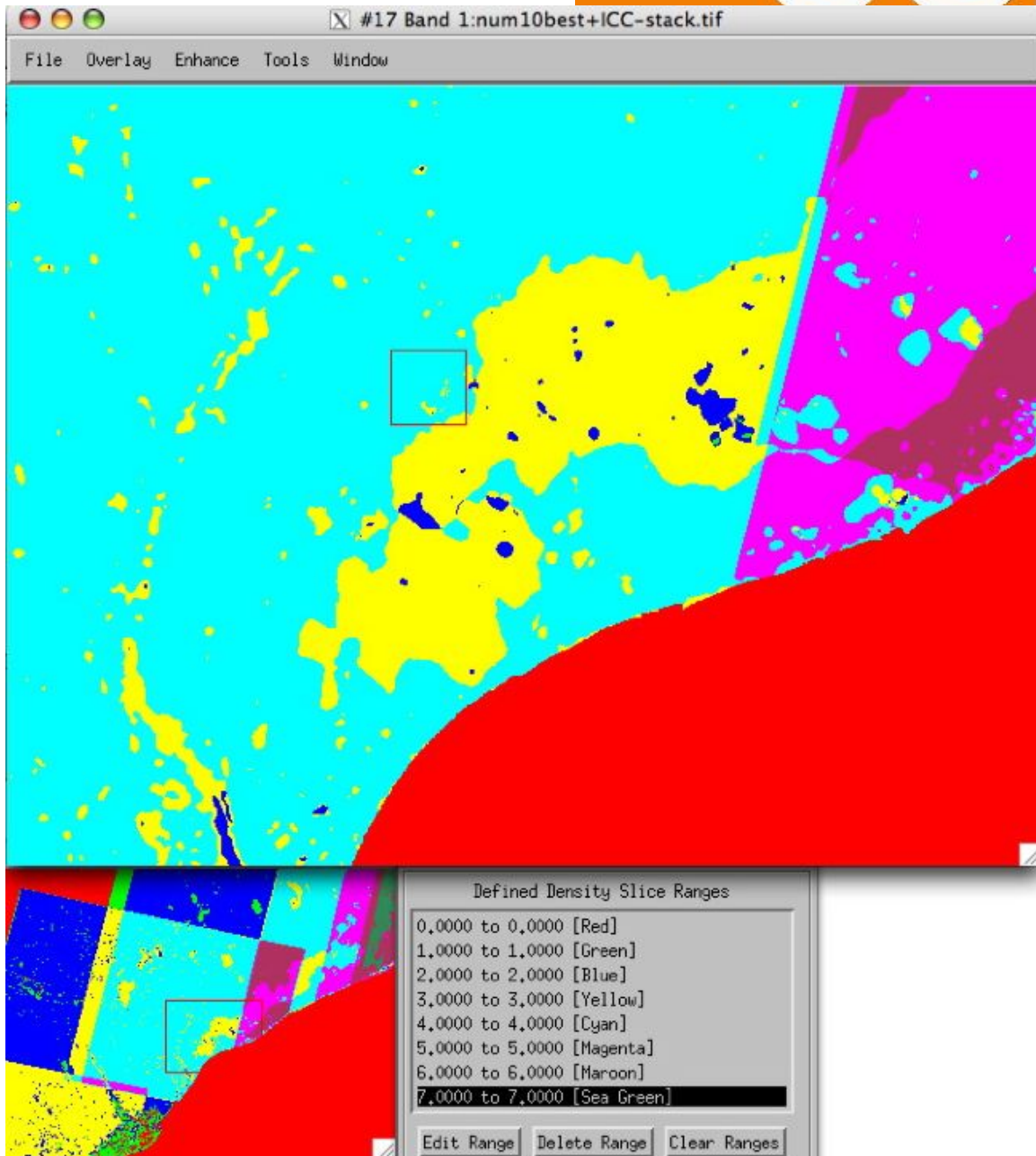
Using the DEM fusion/averaging process, a new DEM was created for the original co-registered DEMs and the cloud and water masked DEMs. The statistics of the differences for the original, masked ASTER vs the mean 10 ASTER (including cloud) and mean 10 ASTER (masking out cloud) are shown in Table 2. There are several intriguing inferences one can draw from this table. Firstly, the effect of clouds is dramatic on the overall bias (15.92->-3.1m) and standard deviation (98.19->17.94m). However, the averaging process, although reducing the bias and standard deviation significantly for the cloudy scene, makes hardly any difference with average difference of individual scenes and the bias and standard deviation of the masked mean 10 DEMs. Unusually, a couple of biases have increased after the masking process. It is not clear what caused this.

ASTER ID	original Bias	original Std.dev.	original Npts	new DIFF-Bias	New DIFF Std.dev.	Npts
1241	-3.00	13.46	2,392,814	3.01	13.36	2,392,157
1240	-2.85	117.68	869,836	-12.95	14.15	861,239
32488	1.58	14.69	871,910	1.54	14.59	871,558
32466	74.21	245.41	2,543,500	6.39	31.14	2,312,514
32402	-4.49	32.91	2,663,999	-5.36	25.52	2,604,791
32314	4.25	48.18	351,767	1.60	28.64	347,303
30732	-6.14	10.17	157,343	-6.14	10.16	157,343
30253	-6.37	25.46	537,743	-7.71	13.48	528,225
30250	106.03	402.57	113,740	0.41	16.25	103,202
29849	-4.00	71.36	2,630,526	-11.75	12.08	2,568,333
	15.92	98.19		-3.10	17.94	
MEAN (all)				8.98	50.26	3,814,875
MEAN (NaN)				-3.15	16.37	3,813,039
SRTM-C				3.56	6.93	3,977,972

**Table 3. Difference elevation statistics for original (with cloud), new (masked cloud) and the overall 10-best mean (with, without cloud) compared to C-SRTM for the Barcelona test site DEMs. All units in metres.**

Only the SRTM, once again, meets the specifications of the DTED-2®. The co-registration of the individual ASTER-DEMs, C-SRTM and reference DEM is within 1 pixel so the differences cannot be ascribed to this cause. It does appear as if matcher noise, specifically spikes due to poor contrast and consequent blunders may be the cause.

It is interesting to observe the complexities of where different DEM elevations come from when merging the data. Figure 15 shows a source image after the masking process. The shapes of the NaN masks is barely discernible in the final product.

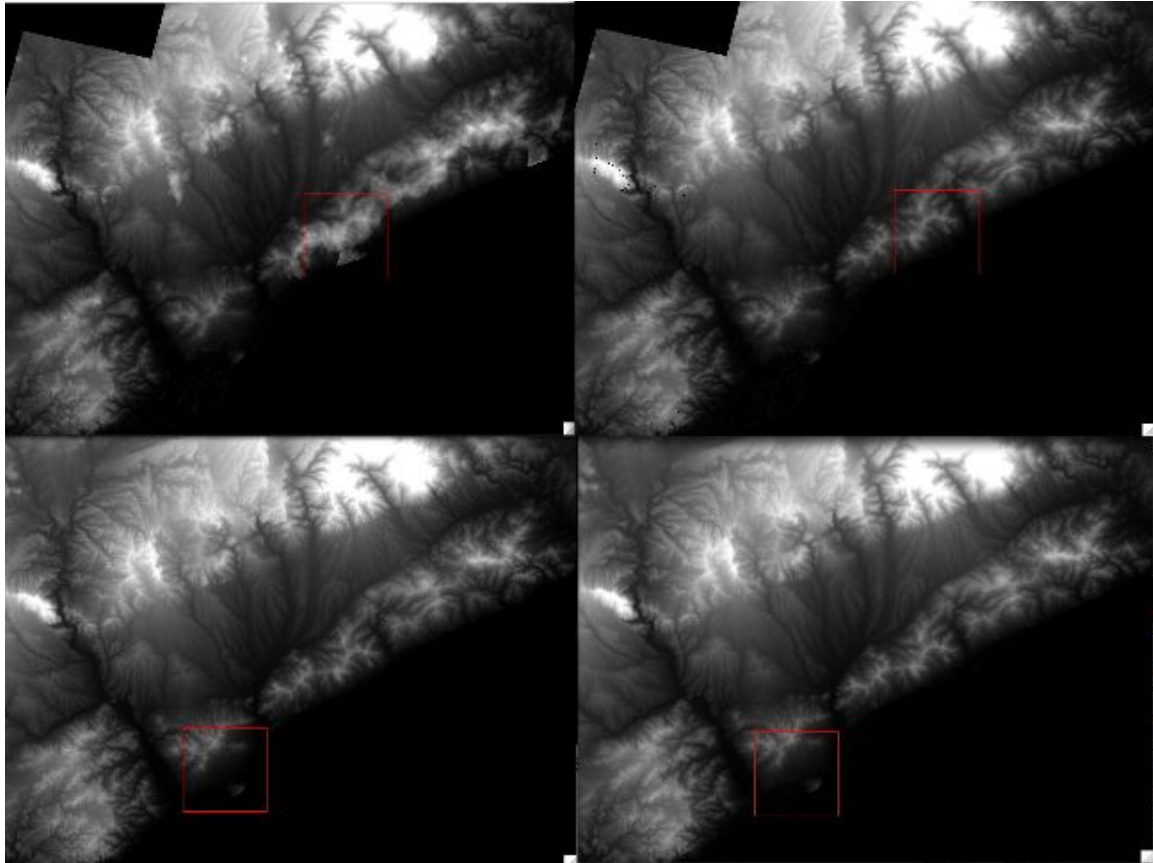


**Figure 15. Number of data layers used for each pixel with the NaN masked input DEMs.**

Finally, the merged DEMs can be viewed in Figure 16 which shows that there is no discernible difference between the reference DEM, the C-SRTM and the merged DEM with the masked DEM inputs. However, the cloudy DEM fusion shows clear artefacts due to clouds. There is therefore a need to develop either a perfect cloud screening system before stacking or use the DEM heights themselves. A simple idea would be to difference each height pixel in the stack layer from all of the other stack layers, rank the results and decide on-the-fly which of these height differences were sensible and which were probably due to clouds or a stereo-matching artefact.

### Concluding remarks

Error characteristics have been demonstrated for ASTER and C-SRTM DEMs with the SRTM meeting the DTED-2® specification (12m Zrms). The merged fused ASTER DEM may just meet the DTED-2® specification if sufficient numbers of input ASTER DEMs are available, planimetric co-registration is good and there are either few clouds or cloud screening are excellent. ASTER DEMs appear to have a good potential as a gap-filler for 30m SRTM DEMs and vice versa. It would be worthwhile in future to explore this further over the CEOS test sites in North America which has much more complex topography, large areas of wetlands and dense tree cover.



**Figure 16. Inter-comparison of DEMs over the Barcelona CEOS-WGCV-TMSG test site. Upper-left: ASTER DEMs merged without screening out clouds, Upper-right, the same process but with the masked DEM inputs. Lower left- reference (ICC) DEM, Lower right- C-SRTM DEM.**

### Acknowledgements

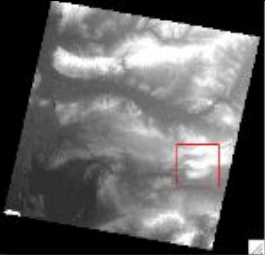
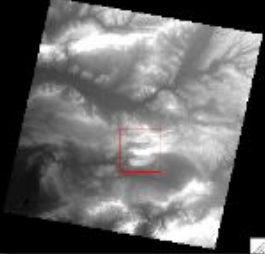
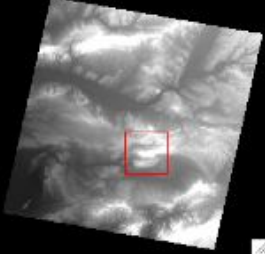
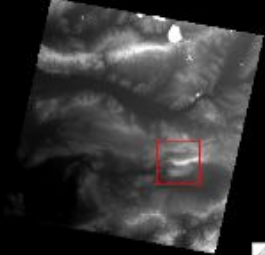
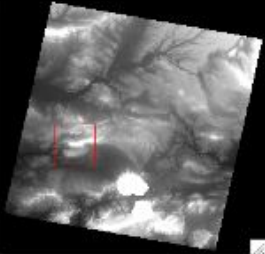
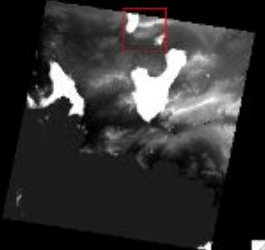
The author would like to thank BNSC for partial funding support and Wyn Cudlip and Rachel Bird of Qinetiq for contract management. The author would also like to thank Wolfgang Kornus (ICC) for the kind loan of the Barcelona DEM, Nick Austin for the implementation of the ASTER-SRTM DEM fusion, John Dwyer (USGS-EDC) for the provision of the Puget Sound NED and co-registered SRTM (not shown here) and Mike

Pitkin for the production of the AeP DEM which has played such an important role over the last 20 years of research. The author would also like to thank Dr Jung-Rack Kim for developing the IDL code to work around the ENVI and IMAGINE NaN “features”, Dr Shih-Yuan Lin for computing the multi data layer statistics using this code and Jeremy Morley (UCL-CEGE) and Brian Bailey (USGS-EDC) for helpful discussions.

### References cited

- Austin, N. J., J.-P. Muller, G. Lixia, and J. Zhang, 2008: A Regional Investigation of Urban Land Use Change in the Three Gorges Reservoir Area, People's Republic of China: Zigui to Wanzhou. *International Journal of Remote Sensing*, **submitted (4/08)**.
- Buckley, S. J. and H. L. Mitchell, 2004: Integration, validation and point spacing optimisation of digital elevation models. *The Photogrammetric Record*, **108**, 277-295.
- Fujisada, H., G. B. Bailey, G. G. Kelly, S. Hara, and M. J. Abrams, 2005: ASTER DEM performance. *IEEE Geoscience and Remote Sensing*, **43**, 2707-2714.
- Grohman, G., G. Kroenung, and J. Strebeck, 2006: Filling SRTM voids: The delta surface fill method. *Photogrammetric Engineering And Remote Sensing*, **72**, 213-216.
- Guth, P. L., 2006: Geomorphometry from SRTM: Comparison to NED. *Photogrammetric Engineering And Remote Sensing*, **72**, 269-277.
- Kelindorfer, J., 2007: Evaluation of the horizontal resolution of SRTM elevation data. *Photogrammetric Engineering and Remote Sensing*, **73**, 336-336.
- Reuter, H. I., A. Nelson, and A. Jarvis, 2007: An evaluation of void-filling interpolation methods for SRTM data. *International Journal of Geographical Information Science*, **21**, 983-1008.
- Weydahl, D. J., J. Sagstuen, O. B. Dick, and H. Ronning, 2007: SRTM DEM accuracy assessment over vegetated areas in Norway. *International Journal of Remote Sensing*, **29**, 3513-3527.

**Appendix 1. Aix en Provence ASTER DEMs**

Filename UTM for (1,1)	NS x NL	Comment (s)	#	Browse images
AST14DMO_00309242007104121_20071128090919_13567_SH.tif  653110.464 E, 4870151.546 N	2526 x 2418	No clouds in area of interest	4	
AST14DMO_00309072001104749_20071128090919_13572_SH.tif  669177.843 E, 4867288.250 N	2526 x 2418	No clouds	5	
AST14DMO_00308122003104022_20071128090929_13687_SH.tif  668231.037 E, 4867397.142 N	2514 x 2412	No clouds	6	
AST14DMO_00307062007104120_20071127232747_30865_SH.tif  658855.079 E, 4869037.676 N	2514 x 2412	No clouds within test site	7	
AST14DMO_00307022000105629_20071128090919_13563_SH.tif  687756.306 E, 4863984.875 N	2544 x 2418	No clouds within test site but noise spikes	7	
AST14DMO_00306292007103515_20071128090939_13868_SH.tif  668651.57 E, 4830482.97 N	2508 x 2388	Large clouds cover much of test-site	9	



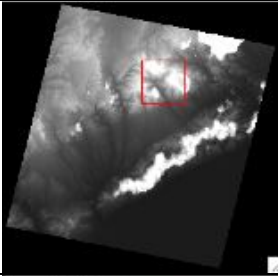
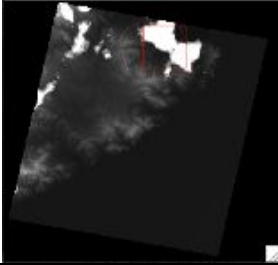
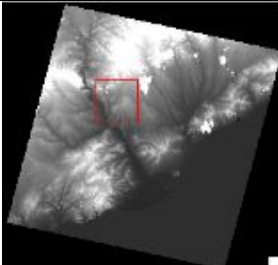
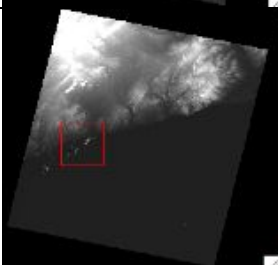
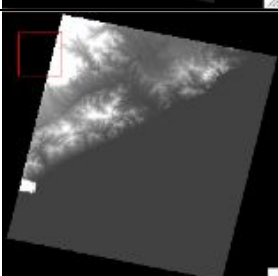
AST14DMO_00306292007103507_20071128090929_13705_SH.tif  680865.945 E, 4889579.638 N	2508 x 2388	Large cloud and most of test-site cut-off	1 0	
AST14DMO_00305062005103445_20071128090929_13701_SH.tif  667045.189 E, 4830697.39 N	2508 x 2388	No clouds	1 1	
AST14DMO_00305062005103436_20071128090929_13699_SH.tif  679274.249 E, 4889789.515 N	2508 x 2388	Possible cloud in SE and most of the test-site is not covered	1 2	
AST14DMO_00304082004104059_20071128090929_13693_SH.tif  668799.168 E, 4867296.231 N	2514 x 2412	No obvious clouds over the test site	1 1	

The following 2 ASTER DSMs did not cover the test site:

AST14DMO\_00306262006103438\_20071128004622\_15463\_SH.tif

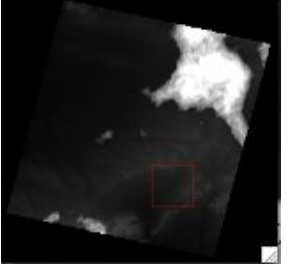
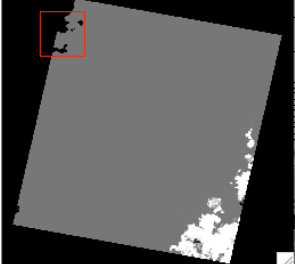
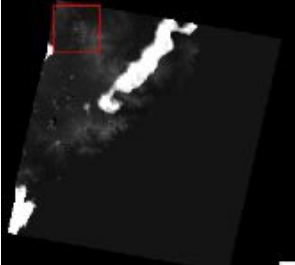
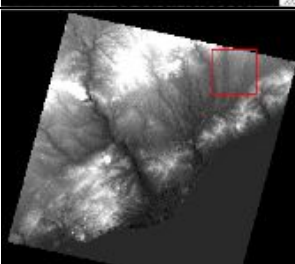
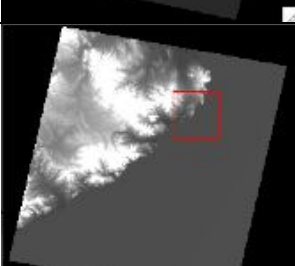
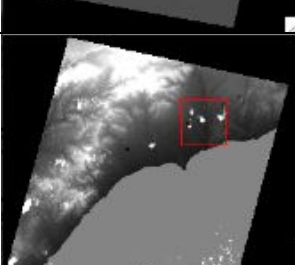
AST14DMO\_00306262006103447\_20071128004622\_15465\_SH.tif

**Appendix 2. Barcelona ASTER DEM characteristics**

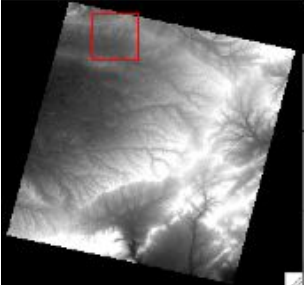
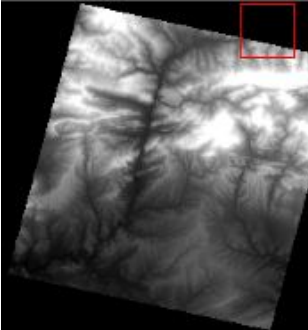
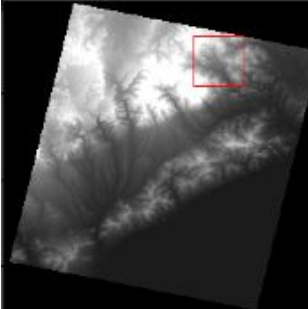
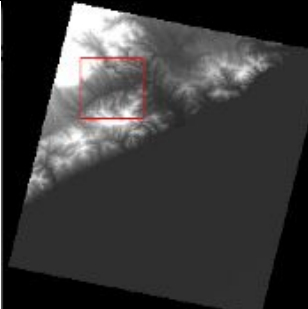
Filename UTM for (1,1)	NS x NL	Comments	#	Browse images
AST14DMO_00310192002104902_20071128143806_32466_SH.tif  407075.5590 E, 4646076.4254 N	2550 x 2442	Clouds along the coast and in the NE	2	
AST14DMO_00309232001104750_20071128143736_32314_SH.tif  458811.3990 E, 4659610.7377 N	2580 x 2424	Clouds in the NE	3	
AST14DMO_00307032001110209_20071128142936_29849_SH.tif  381766.7695 E, 4626239.3488 N	2598 x 2472	Scattered clouds	4	
AST14DMO_00306162003104817_20071128143126_30253_SH.tif  352109.9566 E, 4595483.7757 N	2574 x 2448	Small amount of scattered line clouds	5	
AST14DMO_00306132002104932_20071128143947_1240_SH.tif  439310.2467 E, 4639762.7027 N	2538 x 2442	Clouds in SW corner	6	





<p>AST14DMO_00306072003105426_20071128143858_401_SH.tif</p> <p>439310.2467 E, 4639762.7027 N</p>	<p>2568 x 2472</p>	<p>Large clouds in NE</p>	<p>7</p>	
<p>AST14DMO_00305082003104208_20071128143126_30258_SH.tif</p> <p>453448.2947 E, 4599388.6899 N</p>	<p>2580 x 2424</p>	<p>Sea-only DEM, no land pixels</p>	<p>8</p>	
<p>AST14DMO_00305082003104200_20071128143126_30250_SH.tif</p> <p>453448.2947 E, 4599388.6899 N</p>	<p>2580 x 2424</p>	<p>Coastal line clouds</p>	<p>9</p>	
<p>AST14DMO_00304012002105535_20071128143756_32402_SH.tif</p> <p>381859.6672 E, 4626283.5983 N</p>	<p>2604 x 2478</p>	<p>Small scattered clouds in SW</p>	<p>10</p>	
<p>AST14DMO_00303212003104230_20071128143258_30732_SH.tif</p> <p>465372.7906 E, 4658433.3795 N</p>	<p>2580 x 2424</p>	<p>No obvious clouds</p>	<p>11</p>	
<p>AST14DMO_00303192003105459_20071128172158_6519_SH.tif</p> <p>298453.0242 E, 4582483.3646 N</p>	<p>2568 x 2466</p>	<p>Scattered Cu clouds over land and sea</p>	<p>12</p>	



<p>AST14DMO_00303192003105450_20071128171658_5130_SH.tif</p> <p>314100.9227 E, 4640805.8052 N</p>	<p>2568 x 2466</p>	<p>No obvious clouds</p>	<p>1 3</p>	
<p>AST14DMO_00303192003105442_20071128172028_6112_SH.tif</p> <p>329710.0083 E, 4699133.0094 N</p>	<p>2568 x 2466</p>	<p>No obvious clouds</p>	<p>1 4</p>	
<p>AST14DMO_00303122003104835_20071128143947_1241_SH.tif</p> <p>410634.7699 E, 4645370.1626 N</p>	<p>2550 x 2442</p>	<p>No obvious clouds</p>	<p>1 5</p>	
<p>AST14DMO_00302082003104903_20071128143816_32488_SH.tif</p> <p>439537.4657 E, 4639702.3730 N</p>	<p>2538 x 2442</p>	<p>No obvious clouds</p>	<p>1 6</p>	
<p>AST14DMO_00302022004105440_20071128143736_32312_SH.tif</p> <p>439537.4657 E, 4639702.3730 N</p>	<p>2538 x 2442</p>	<p>No obvious clouds</p>	<p>1 7</p>	